XV Reunión de Trabajo en Procesamiento de la Información y Control, 16 al 20 de septiembre de 2013

Multifractal classification of bread crumb images

Rodrigo Baravalle†, Juan Carlos Gómez† y Claudio Delrieux‡

†*Laboratorio de Sistemas Dinámicos y Procesamiento de Información*
FCEIA, Universidad Nacional de Rosario, - CIFASIS - CONICET
{*baravalle,gomez*}*@cifasis-conicet.gov.ar*
‡*DIEC, Universidad Nacional del Sur - IIIE-CONICET*
cad@uns.edu.ar

Abstract— **Adequate models of the bread crumb structure can be critical for understanding flow and transport processes in bread, creating synthetic bread crumb images for photo-realistic rendering, evaluating similarities and establishing quality features of different bread crumbs types.**

In this article multifractal analysis, employing the multifractal spectrum (MFS), has been applied to classify among different bread crumb types. Four varieties of breads (*baguette*, *sliced*, *bran*, and *sandwich*) were analyzed. Results demonstrate that the MFS based classification is able to distinguish among different bread crumbs with very high accuracy. The MFS has shown to provide local and global image features that are both robust and low dimensional, leading to feature vectors that capture essential information for classification tasks. Multifractal modeling of the bread crumb structure can be an appropriate method for parameterizing and simulating the appearance of different bread crumbs.

Keywords— **multifractal, bread, classification**

1 INTRODUCTION

One of the most important factors to evaluate the quality of a bread loaf is related to its crumb structure. Close examination of different slices reveals considerable variation in the cell (air bubble) size even within a single sample of the same bread type.

Fractal and multifractal analysis of images have proved to be able to capture useful properties of the underlying material being represented. These features have been successfully applied in different areas, such as medicine [1, 2] and texture classification [3]. In food research, fractal and multifractal analysis has been applied in the study of apple tissues [4], pork sirloins [5], and also in chocolate, potato and pumpkin surfaces [6]. Through several procedures [7, 8], it is possible to obtain different Fractal Dimensions (FD), each of them capturing a different property of the material (*e.g.*, porosity, rugosity).

For each material, the results obtained in classification tasks are useful in quality measurements of real samples and also in the validation of synthetic representations of them. In other words, these processes are useful to determine if a given image presents the observed features in that material, allowing to associate quality measure parameters to it. In [9], a bread crumb quality test based on Gabor filters was performed, obtaining good results. Nevertheless, a small database was used (30 images). In [8] several fractal features were obtained for one type of bread, demonstrating that a vector of FDs would be capable of obtaining key features of the crumb texture more accurately than using a single FD.

In this work we propose the application of the Multifractal Spectrum (MFS) [10] to classify different bread crumb types. One of the main features of the MFS is its bi-Lipschitz invariance, that is, invariance to perspective transforms (viewpoint changes) and smooth texture surface deformations. It is shown that the MFS is also locally invariant to affine changes in illumination.

The proposed method is compared to other classifiers that use state-of-the-art features for texture classification. The results of this feature extraction procedure show that the classifier is robust and presents good discrimination properties to distinguish between different bread types and also bread from non bread images.

This paper is organized as follows. In section 2 the theory underlying fractal sets is introduced, and the materials and methods employed in this work are presented. In section 3 the results obtained in the classification procedures are shown and discussed. In section 4 the conclusions are summarized, as well as possible future works.

2 MATERIALS AND METHODS

2.1 Fractals and Multifractals

The term *fractal* was first employed by the mathematician B. Mandelbrot in [11]. Fractal objects have the property of self-similarity (*i.e.*, the geometrical or topological properties are invariant at different scales), and they are characterized by a non-integer dimension. Fractal objects can have one or more FDs. Most of the famous fractal sets (*i.e.*, the Cantor set, the Von Koch curve, and the Sierpinsky gasket) can be characterized by a single exponent that relates how their geometrical properties vary under scale changes. On the other hand, there are cases where the fractal object exhibits different exponents under different scales. Those are called *multifractals* [12], and are characterized by a sequence of FDs, or even a

function that establishes how is the local variance of the geometrical properties under scale changes. It is assumed that these structures are composed by different fractals coexisting simultaneously. The result is a vector containing several FDs. The multifractal approach characterizes better the objects than the fractal one, since variations in local regions are captured in a more accurate manner. The following definition is used in fractal and multifractal measurements.

2.1.1 Box Dimension

On the one hand, mathematical objects such as the Koch curve and the Sierpinski triangle have exact self-similarity. Natural phenomena, on the other hand, are better described by statistical self-similarity. In such cases, the Box FD is used. Box FD is a simplification of the Hausdorff (originally Minkowski - Bouligand) dimension for non strictly self-similar objects [7]. Given a binarized image, it is subdivided in a grid of size $M \times M$ where the side of each box formed is ϵ. If N_ϵ represents the amount of boxes that contains at least one pixel in the binarization of the set for that ϵ, then the box dimension D_b is defined as

$$D_b \triangleq \lim_{\epsilon \to 0} \frac{\log(N_\epsilon)}{\log(1/\epsilon)}. \quad (1)$$

The algorithm uses a binarized image and selects different values of ϵ in it, making a count of the boxes that contains pixels in each case (to avoid numerical instabilities, a mean of cases is computed, establishing different positions in the grid over the image). Finally, a linear regression adjustment is made with the obtained data, in the $\log - \log$ space, and the slope of the straight line is by definition the box dimension of the image. In Fig. 1 an image of the bread type *bran* is shown with its corresponding box dimension computation.

2.2 The theory behind Multifractal Analysis

In [8], several procedures were applied to analyze the bread crumb structure. In that paper, it was shown that a vector of FDs could better characterize those structures. Based on that assumption, in this work multifractal analysis of the bread crumb is carried out. The idea behind multifractal analysis is to examine, in the limit, the local behavior of a measure μ at each point of the set under study, this means, to find the Hölder exponent α in that point (see below). The *multifractal spectrum* $f(\alpha)$ (MFS) is obtained applying this procedure to the entire set, in this case, an image.

Let E be an structure divided in disjoint substructures E_i of size ϵ in such a way that

$$\bigcup_i E_i = E. \quad (2)$$

Each substructure E_i is characterized by a measure $\mu(E_i)$. From the point of view of multifractal analysis, it is useful to define the Hölder exponent, α_i, for each substructure E_i, as a function of ϵ, *i.e.*

$$\alpha_i \triangleq \frac{ln(\mu(E_i))}{ln(\epsilon)}, \quad (3)$$

and to take the limit when ϵ tends to 0. The limit represents the value of the Hölder exponent at a point in the structure, that is

$$\alpha = \lim_{\epsilon \to 0} \alpha_i. \quad (4)$$

The exponent characterizes the local regularity of the structure at a point. To obtain a global characterization of the regularity of the structure it is necessary to obtain the distribution of α in E. The range of Hölder exponent values found in the image is partitioned in M sub-ranges (in practice, M is a parameter: the number of FDs). Each α_i defines one sub-range. Then a counting N_ϵ of boxes characterized by α_i must be done for each of them, related to the value of ϵ, *i.e.*

$$f_\epsilon(\alpha_i) = -\frac{ln(N_\epsilon(\alpha_i))}{ln(\epsilon)}. \quad (5)$$

When ϵ tends to 0, the limiting value is the FD of the structure E characterized by α, the Hausdorff dimension (which is calculated by using the Box procedure described) of the α distribution, also known as the *multifractal spectrum* $f(\alpha)$ (MFS) [13], *i.e.*

$$f(\alpha) = \lim_{\epsilon \to 0} f_\epsilon(\alpha). \quad (6)$$

2.2.1 Practical procedure for the MFS

There are several techniques described in the literature to obtain the MFS, which lead to different representations of the multifractal information present in the structure. Usually, the method of moments is used [4, 5], but it produces a feature vector which is not always suitable for classification tasks. In this work, the implementation presented in [10] is employed, due to its better classification performance. The implementation first calculates the method of moments and then uses a Legendre transform to obtain the MFS. The procedure consists in partitioning the domain into non-overlapping boxes of length r. The q-th moment of a measure μ is defined as

$$M_r(q) = \sum \mu(B(x,r))^q, \quad (7)$$

where the sum is over the r mesh squares for which $\mu(B(x,r)) > 0$. To denote the power law behavior of $M_r(q)$, $\beta(q)$ is defined as a straight line fit of the values $M_r(q)$ with respect to r, for r in $1, .., n$. It is shown in [14], that the MFS and $\beta(q)$ are related to each other by a Legendre transform as

$$f(\alpha(q)) = q\alpha(q) - \beta(q), \quad (8)$$

where

$$\alpha(q) = \frac{d\beta(q)}{dq}. \quad (9)$$

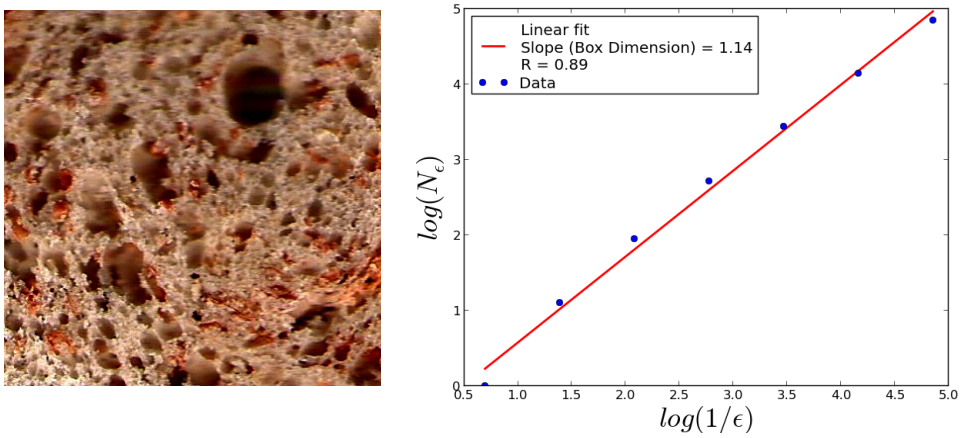

Figure 1: An image and its computed box dimension

As previously stated, the $f(\alpha)$ spectrum (MFS) and the generalized dimensions $\beta(q)$ contains the same information, but in this work the first is employed, since it also outperforms the method of moments in classification tasks. Using (8) and (9) the MFS is estimated. As previously said, in this work the implementation in [10] is used and the parameters of the algorithm are set to default (except for the number of FDs, since they are chosen based on its classification performance).

2.2.2 *Multifractal Measures*

Defining different μ functions counts for different image features. The first approach is to define μ in the intensity domain, *i.e.*

$$\mu(B(x,r)) = \int_{B(x,r)} (G_r * I)dx, \qquad (10)$$

where $*$ is the $2D$ convolution operator and G_r is a Gaussian smoothing kernel with variance r, *i.e.,* μ is the weighted average intensity value in the disk of radius r centered at x $(B(x,r))$. This is the density of the intensity function, and it describes how the intensity at a point changes over scale.

The definition of μ could serve to specific purposes. For instance, if robustness to illumination changes is needed, one choice is to define $\mu(B(x,r))$ on the domain of the energy of the gradients. Let $f_k, k = 1,2,3,4$ be four directional differential operators along the vertical, horizontal, diagonal and anti-diagonal directions. Then we define the measurement function $\mu(B(x,r))$ for the image I as in (11).

$$\mu(B(x,r)) = (\int_{B(x,r)} \sum_k (f_k * (G_r * I))^2 dx)^{1/2}. \qquad (11)$$

Another choice is to define $(B(x,r))$ as the sum of the Laplacians of the image inside $B(x,r)$ (12).

$$\mu(B(x,r)) = \int_{B(x,r)} |\nabla^2 (G_r * I)|dx. \qquad (12)$$

2.3 Image Acquisition

Twenty images of 4 different commercial bread types (*sliced*, *baguette*, *bran* and *sandwich*), counting 80 images, were obtained in the same day of purchase using an HP PSC 1210 scanner with the following settings: highlight 190, shadows 40, and midtones 1, and they were saved in TIFF format. Images showed a resolution of 380×380 pixels (the maximum possible area for the four bread types) and 350 dpi (1 pixel $= 0.00527mm^2$). Then the images were converted to gray scale (8 bits). In addition, 20 images of each bread type were acquired with a digital camera, using the same spatial resolution, counting 80 images. The illumination conditions of these images were different from that of the scanner in order to test for the robustness of the method. We also employed one hundred randomly selected images from the CalTech101 [15] dataset in order to test the method's performance with non-bread images. In Fig. 2 three examples of the images used in this paper are shown. In the figure, 2 images of the *baguette* bread type, digitalized using a scanner (left) and a digital camera (center) are shown with a random non bread image from the Caltech101 dataset (right).

3 RESULTS AND DISCUSSION

3.1 Data Analysis

The MFS, using 20 FDs, was applied for each of the 200 images (*i.e.,* 40 images of each bread type, and 40 randomly selected nonbread images, getting 5 balanced classes).

Self-organizing maps (SOM) [16] of the vectorized images are useful to visualize these different representation of bread images into a lower dimensional view, in order to understand them better. A SOM map high dimensional data into a (typically) two-dimensional representation, using neighborhood information. Topological information of the original data is preserved.

Unsupervised SOM of the multifractal representation of bread and non-bread images are shown in Fig. 3 in a

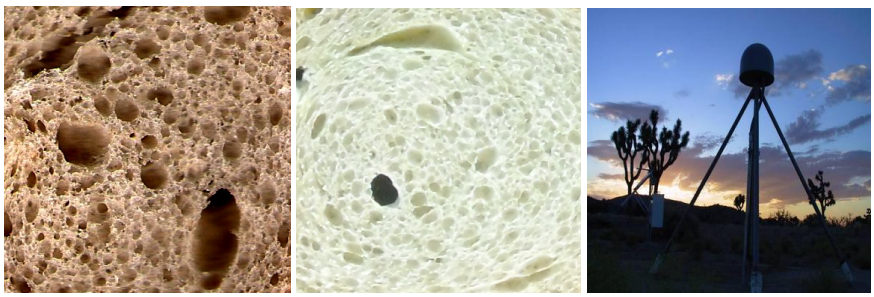

Figure 2: Digitalized images of *baguette* bread type and an image of the CalTech101 dataset

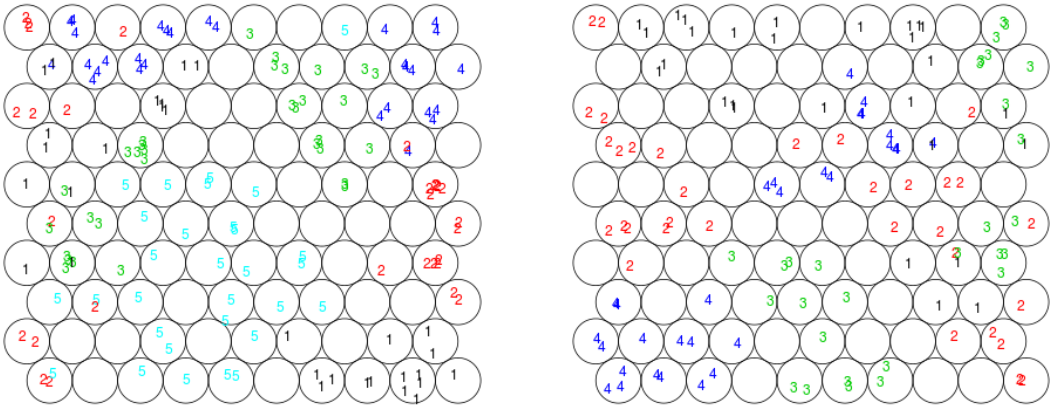

Figure 3: SOM of the bread and non-bread vectorized images (left) and SOM of the vectorized bread images only (right). 1: *baguette*, 2: *sliced*, 3: *bran*, 4: *sandwich*, 5: *nonbread*

grid of 10×10 cells. In the left image, the 5 classes (*e.g.*: *baguette*, *sliced*, *bran*, *sandwich* and *nonbread*) are shown, while in the right image, the *nonbread* class has been removed, and then the SOM was recomputed for the remaining four classes, in order to highlight details among the MFS of the different bread types. The multifractal features SOM appears to show easily separable classes. It seems that a classifier could potentially obtain low classification errors using the multifractal features.

3.2 Bread Classification

As previously stated, five classes are defined, *e.g.*, *baguette*, *sliced*, *bran*, *sandwich* and *non-bread*, assigning 40 images to each class. A comparison is made between the MFS and state-of-the-art features in the computer vision literature. This classification schema corresponds to an intra-class problem, which is harder to solve than an ordinary inter-class one.

K-fold cross validation is applied to the entire set (with $K = 4$), employing three different classifiers: Support Vector Machines (SVM), Random Forests (RF), and Nearest Neighbors (NN). Results show that the MFS presents good classification performance regardless of the classifier employed. The libsvm implementation [17] was used for the SVM classifier (with RBF kernel). In the case of the RF (100 trees) and the NN (1 neighbor) classifiers, the scikit-learn python library was employed.

In Table 1, the classification performance of the method is tested using different numbers of FDs. When 20 FDs are used, an useful combination of performance and low dimensionality is achieved, so this number of FDs is used in the following calculations.

In Table 2, several combinations of different MFS obtained from the images, and their classification performance are shown. The MFS used in the study were the density of the intensity (MFS in the table), the Laplacian of the intensity (L), and the gradient of the intensity (G). In addition, another test is made, using the CIELab color space. The key advantage of this color space is that it tends to reduce the dependency of the resulting image color on the device used in the capture. The intensity of the images is transformed to the CIELab space, and the MFS of the three separated channels (L, a, and b) are combined together, obtaining a vector of 60 FDs. This combination showed the best classification performance. It means that adding color information in the a and b channels is useful for better classification of different types of bread crumbs, when different capturing

devices are used (in this case, a scanner and a digital camera).

In Table 3, state-of-the-art features (Haralick, Local Binary Pattern and SIFT features) are computed for the images. The Haralick and Local Binary Pattern features are computed using the *mahotas* (https://pypi.python.org/pypi/mahotas) python library. The best classification performance is obtained using the SIFT features, but a 128 feature length vector is obtained per image, and, in addition, computational space and time is needed to build internal structures (*e.g.* a *codebook*). The classification performance of the MFS for the bread crumb database is the highest among the algorithms studied. The MFS captures robust and useful information for classification in low dimensional features. These results also agree with results obtained in [18] for the classification of other food products.

Table 1: classification results with different number of FDs for the MFS

SVM	**96%**	94.5%	95.5%
RF	91.5%	**93.5%**	93%
NN	88.5%	**90.5%**	90%
#FDs	10	20	30

Table 2: classification results using different combinations of the MFS

Method	MFS	MFS+L	MFS+G	CIELab
SVM	94.5%	95.5%	**97.5%**	**97.5%**
RF	93.5%	**96%**	95%	**96%**
NN	90.5%	90%	87%	**92%**
#FDs	20	40	40	60

Table 3: classification results for different features

Method	Haralick	Lbp	SIFT
SVM	94%	78.5%	**96.5%**
RF	91%	71.5%	**92%**
NN	79%	70%	**86%**
#Features	13	36	128

4 CONCLUSIONS

The use of multifractal features in bread crumb texture classification showed excellent performance. The MFS demonstrated to be accurate enough to perform a classification of different bread types and also to discriminate non bread from bread images. The classification performance of the MFS for the bread crumb database outperforms other state-of-the-art techniques employed in the computer vision literature. The information present in the MFS of the L, a and b channels of the CIElab space color obtained the best classification performance in all the developed tests. This result appears to be a consequence of the different capturing devices used in this work.

The results found could also be applied to validate synthetic samples, in the sense that they should have similar features to the bread type they are trying to simulate. The features found with the MFS could be applied to tune bread crumb quality parameters.

References

[1] J. Andjelkovic, N. Zivic, B. Reljin, V. Celebic, and I. Salom, "Classifications of digital medical images with multifractal analysis," in *Proceedings of the 8th conference on Signal, Speech and image processing*, ser. SSIP'08. Stevens Point, Wisconsin, USA: World Scientific and Engineering Academy and Society (WSEAS), 2008, pp. 88–92.

[2] L. Yu and D. Qi, "Holder exponent and multifractal spectrum analysis in the pathological changes recognition of medical ct image," in *Control and Decision Conference (CCDC), 2011 Chinese*, may 2011, pp. 2040 –2045.

[3] H. Wendt, P. Abry, S. Jaffard, H. Ji, and Z. Shen, "Wavelet leader multifractal analysis for texture classification," in *16th IEEE International Conference Image Processing (ICIP)*, nov. 2009, pp. 3829 –3832.

[4] F. Mendoza, P. Verboven, Q. T. Ho, G. Kerckhofs, M. Wevers, and B. Nicolaï, "Multifractal properties of pore-size distribution in apple tissue using x-ray imaging," *Journal of Food Engineering*, Feb. 2010.

[5] S. Serrano, F. Perán, F. J. Jiménez-Hornero, and E. Gutiérrez de Ravé, "Multifractal analysis application to the characterization of fatty infiltration in iberian and white pork sirloins." *Meat Sci*, vol. 93, no. 3, pp. 723–732, 2012.

[6] R. Quevedo, L.-G. Carlos, J. M. Aguilera, and L. Cadoche, "Description of food surfaces and microstructural changes using fractal image texture analysis," *Journal of Food Engineering*, vol. 53, no. 4, pp. 361 – 371, 2002.

[7] H. O. Peitgen, H. Jürgens, and D. Saupe, "Chaos and fractals: new frontiers of science," 2004.

[8] U. Gonzales-Barron and F. Butler, "Fractal texture analysis of bread crumb digital images," *European Food Research and Technology*, vol. 226, pp. 721–729, 2008.

[9] Y. Fan and H. Zhang, "Application of gabor filter and multi-class svm in baking bread quality classification," in *Mechatronics and Automation, Proceedings of the 2006 IEEE International Conference on*, june 2006, pp. 1498 –1502.

[10] Y. Xu, H. Ji, and C. Fermuller, "A projective invariant for textures," in *Computer Vision and Pattern Recognition, 2006 IEEE Computer Society Conference on*, vol. 2, pp. 1932–1939.

[11] B. B. Mandelbrot, *The Fractal Geometry of Nature*. New York: W. H. Freedman and Co., 1983.

[12] B. B. Mandelbrot, "Multifractal measures, especially for the geophysicist," *Pure and Applied Geophysics*, vol. 131, pp. 5–42, Mar. 1989.

[13] A. Silvetti and C. Delrieux, "Multifractal analysis of medical images." ser. Actas de la trigésimo novena Jornada Argentina de Informática e Investigación Operativa (JAIIO), 2010, pp. 1575 – 1581.

[14] K. J. Falconer, *Techniques in Fractal Geometry*. John Wiley, 1997.

[15] L. Fei-Fei, R. Fergus, and P. Perona, "Learning generative visual models from few training examples an incremental bayesian approach tested on 101 object categories," in *Proceedings of the Workshop on Generative-Model Based Vision*, Washington, DC, June 2004.

[16] T. Kohonen, M. R. Schroeder, and T. S. Huang, Eds., *Self-Organizing Maps*, 3rd ed. Secaucus, NJ, USA: Springer-Verlag New York, Inc., 2001.

[17] C.-C. Chang and C.-J. Lin, "LIBSVM: A library for support vector machines," *ACM Transactions on Intelligent Systems and Technology*, vol. 2, pp. 27:1–27:27, 2011.

[18] M. Bosch, F. Zhu, N. Khanna, J. Boushey Carol, and E. J. Delp, "Food texture descriptors based on fractal and local gradient information," in *European Signal Processing Conference*, ser. EUSIPCO 2011, 2011.